SUPPLEMENT TO THE *WELDING JOURNAL*, SEPTEMBER 2012
Sponsored by the American Welding Society and the Welding Research Council

Study on Vacuum Brazing of Glass to Kovar® Alloy with Cu-Ni-Sn-P

The optimum brazing time and temperature were sought to improve the shear strength and hermetic seal in the fabrication of a solar power system

BY Z. ZHONG, J. ZHOU, X. SHEN, AND X. LING

ABSTRACT

A vacuum brazing process of borosilicate glass to Kovar® alloy was carried out at 943~973 K using Cu-Ni-Sn-P brazing alloy. The shear strength was tested after vacuum brazing, and the microstructural evaluation of the glass-to-metal brazed joints was performed by scanning electron microscopy (SEM), energy-dispersive spectroscopy (EDS), and X-ray diffraction (XRD). The results showed that the maximum shear strength of the brazed joint was 1.6 MPa when the brazing temperature was 953 K and the brazing time was 10 min. The fracture location of the brazed joint was near the side of the glass. Many microcracks occurred along the interface of the glass, and then extended to the center of the interface. Cu_3P and Ni_2P intermetallic compounds, α-Cu, and Cu_xSn_y layer form at the interface of the brazed joint. The compounds Cu_3P and Ni_2P are harmful for the strength of the brazed joint.

Introduction

Glass-to-metal seal technology is applied to fabricate heat receivers, which convert solar energy into thermal energy. A glass-to-metal seal requires a certain mechanical strength and excellent gas tightness under a high-vacuum condition, which become key factors in a parabolic trough solar thermal power system (Ref. 1).

The methods for glass-to-metal sealing can be classified into fusion sealing and diffusion welding. Oxidation treatment of the metal is often done for the two methods to promote the glass-to-metal adhesion, which can provide a transition layer between the metal and the glass (Refs. 2–4). The two following conditions are necessary for a glass-to-metal seal: 1) The coefficients of thermal expansion (CTE) of the metal and glass should be as close as possible in order to reduce thermal stress generated during the cooling from the joining temperature to room temperature, and 2) the metal should have excellent surface wettability with the glass to provide good mechanical adhesion and gas tightness.

Anodic bonding, successfully realized for the first time in 1969 by Wallis and Pomerantz, is a typical diffusion sealing method to seal an alkali-rich glass to any metal. It has been used to join glass and metal by applying a voltage between two samples (Refs. 5, 6). However, the bonding strength and gas tightness of the joints formed using two sealing processes were not good enough to be used in the parabolic trough solar thermal power system (Ref. 7).

Therefore, it is very important to improve the shear strength between the glass and metal. In this research, a vacuum brazing process was used to improve the joint strength and simplify the sealing process. The shear strength of the joints was measured. Scanning electron microscopy (SEM) and X-ray diffraction (XRD) were applied to analyze the microstructure of the joint interface.

Experimental

KEYWORDS

Glass-to-Metal Adhesion
Vacuum Brazing
Microstructure
Shear Strength
Cu-Ni-Sn-P Brazing Alloy

Material

The glass and metal were joined together using vacuum brazing technology. The experimental materials used in this investigation were borosilicate glass 3.3 and Kovar® (iron-nickel-cobalt alloy) because of their similar CTE (Ref. 8). Meanwhile, borosilicate glass has characteristics of chemical stability and anticorrosion at high temperature (Ref. 9). The amorphous Cu-7wt%Ni-9wt%Sn-6wt%P filler metal with the solidus temperature 833 K and the liquidus temperature 913 K was used. Filler metal foils with 50-μm thickness and 6-mm width were fabricated using a rapid solidifying technique (Ref. 10). Tables 1 and 2 show the composition of Kovar alloy and borosilicate glass, respectively. Table 3 lists the mechanical properties of the alloy and glass.

Process

Both borosilicate glass and Kovar® alloy were cut into samples with dimensions of 60 × 20 × 4 mm and 60 × 20 × 1.5 mm, respectively. The joining surface of the Kovar was ground flat by grit paper and cleaned in ethanol and acetone solution (Ref. 11). The joining surface of the borosilicate glass was electroless plated with a thin copper layer. Before the electroless plating, the glass surface was roughened by sand blasting to improve the adhesive ability between the glass substrate and copper layer (Ref. 12). The softening point of borosilicate glass is about 1097 K.

The borosilicate glass, Cu-Ni-Sn-P foils, and Kovar alloy were assembled as shown in Fig. 1. The mating surfaces of samples were kept in contact by a specially designed clamp, and pressure was applied along the longitudinal direction to enhance the interfacial reaction. The specimens were placed into a vacuum brazing furnace. The vacuum was maintained at 4×10^{-2} Pa during the brazing process.

Z.ZHONG, J. ZHOU, X. SHEN, and X. LING are with School of Mechanical and Power Engineering, Nanjing University of Technology, Nanjing, China.

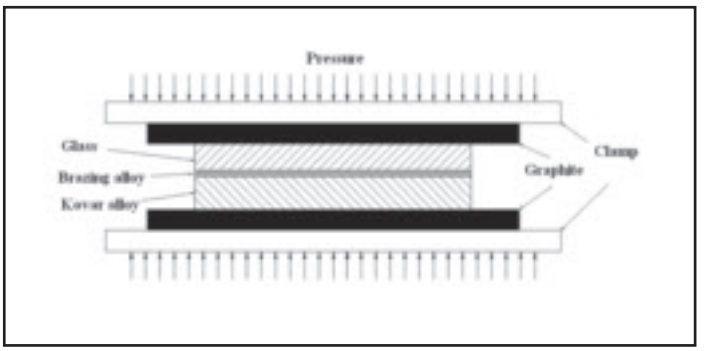

Fig. 1 — Map of the glass-to-metal brazing setting.

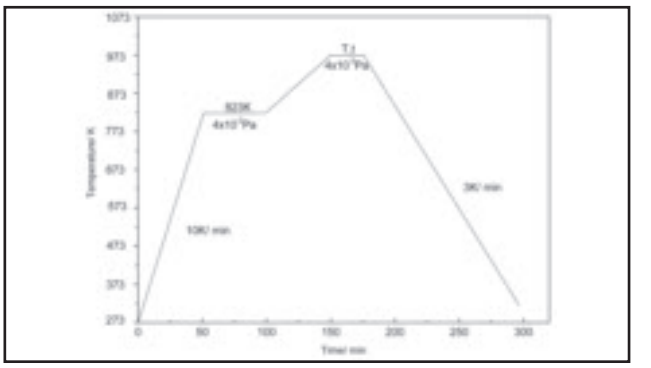

Fig. 2 — Technical requirement graph of the vacuum brazing experiment.

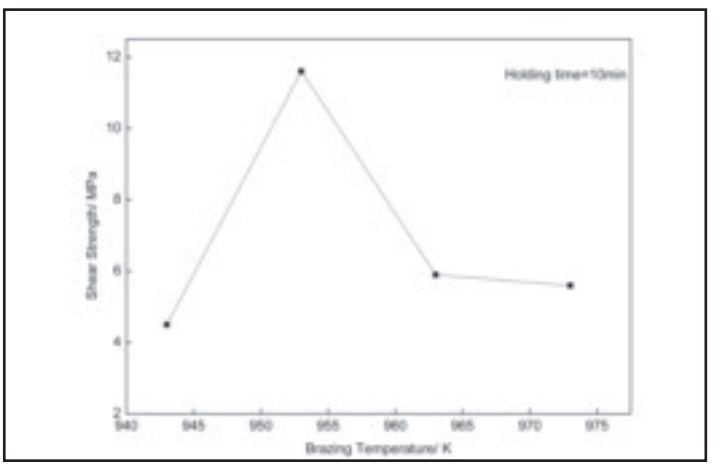

Fig. 3 — Relationship between the brazing temperature and shear strength.

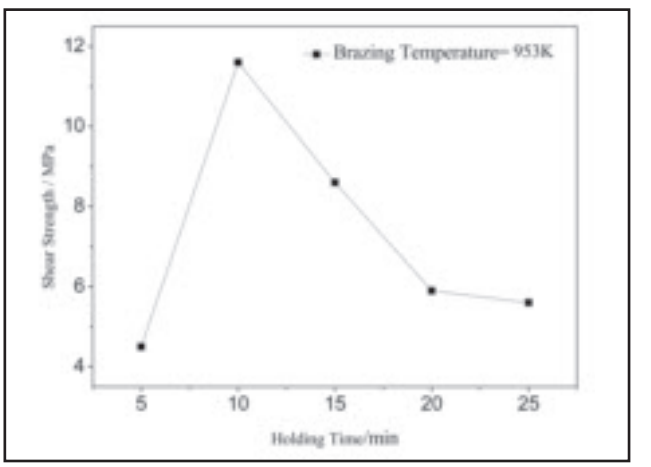

Fig. 4 — Relationship between the brazing time and shear strength.

Then, the specimens were heated to the brazing temperatures of 933, 943, 953, 963, and 973 K, respectively, and the heating rate was 10 K/min. The brazing times were 5, 10, 15, 20, and 30 min, respectively. In order to reduce the brazed residual stresses, the samples were cooled at the rate of 3 K/min from the joining temperature to 573 K and then cooled to room temperature in the furnace. The temperature change during the vacuum brazing experiment is shown in Fig. 2.

After vacuum brazing, shear strengths of five samples were measured at a constant speed of 0.5 mm/min in the MTS testing machine. The average value of five samples was taken as the shear strength. The microstructure of the brazed joint was examined using SEM and XRD to investigate the phase composition in the area of the brazed joint. Meanwhile, the element distribution on the interface was measured using energy-dispersive spectroscopy (EDS).

Results and Discussion

Shear Strength of the Brazed Joint

To obtain the mechanical property of the brazed joint, the shear strength was measured by means of a digital press testing machine. The relationship between the brazing temperature and shear strength is shown in Fig. 3. It can be seen that the brazing temperature has a marked effect on shear strength of the joint. The shear strength gradually increases from 6 to 11.6 MPa when the heating temperature increases from 933 to 953 K. The main reason is that the atom diffusion near the interface can be sufficient to form an excellent metallurgical combination at elevated temperatures. However, shear strength decreases due to coarseness of the microstructure when the brazing temperature continually increases.

The relationship between the brazing time and shear strength is shown in Fig. 4. As shown in Fig. 4, the shear strength of the joint brazed at 953 K rapidly increases with an increase in brazing time, and a brazed joint with a shear strength of 11.6 MPa can be obtained at 953 K for 10 min. However, the shear strength of the brazed joint reduces when the brazing time is longer than 10 min. The brazing time has an important effect on the shear strength of the joint. If the brazing time is shorter than 10 min, the brazing filler metal just melts, and the diffusion of the brazing filler metal and base metal isn't uniform, which leads to the low shear strength of the joint. If the brazing time is longer than 10 min, the brazing filler metal is easily lost and forms brittle compounds, which

Table 1 — Chemical Composition of Kovar Alloy (wt-%)

C	P	S	Mn	Si	Cu	Cr	Mo	Ni	Co	Fe
≤0.03	≤0.02	≤0.02	≤0.5	≤0.3	≤0.3	≤0.2	≤0.2	28.5~29.5	16.8~17.8	base

Table 2 — Chemical Composition of Borosilicate Glass (wt-%)

SiO_2	B_2O_3	Na_2O	Al_2O_3	CaO
80.9	12.7	4	2.3	0.1

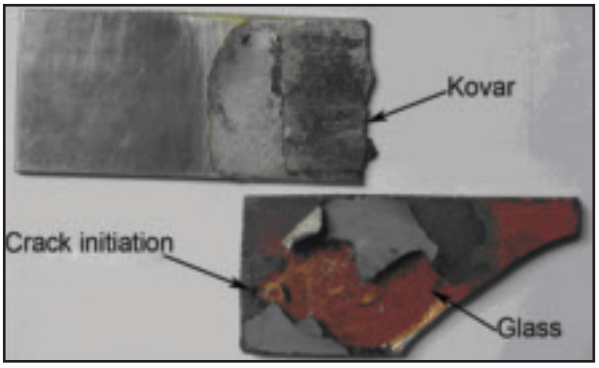

Fig. 5 — Macromorphology of shear crack on a brazed joint.

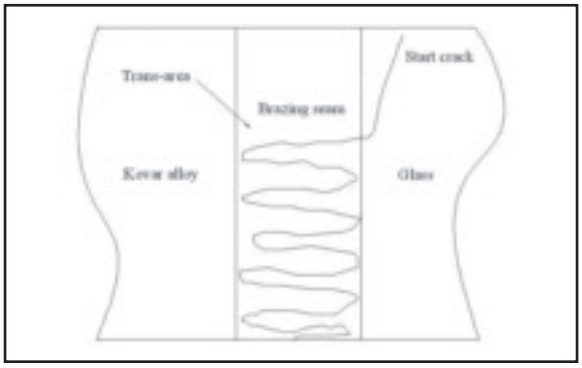

Fig. 6 — Map of rupture crack path of a brazed joint.

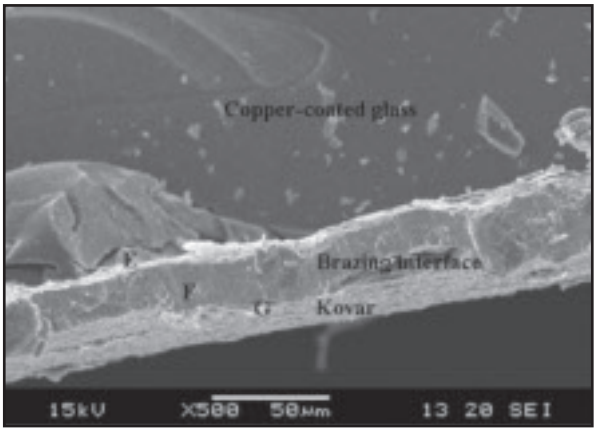

Fig. 7 — Microstructure of the joining interfaces for glass/brazing alloy/Kovar alloy.

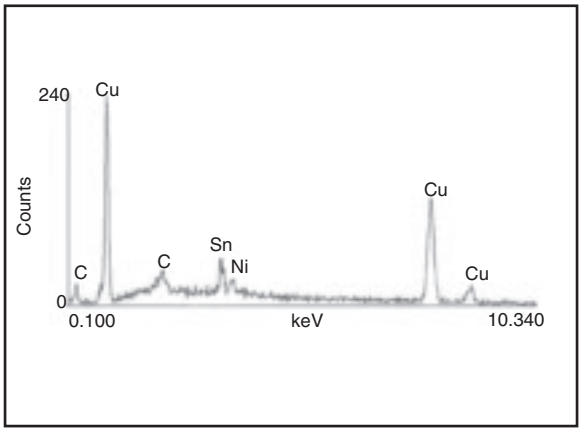

Fig. 8 — EDS analysis of a small area component of the glass-to-brazing alloy interface (Region E).

make the shear strength of the joint decrease. Therefore, it is necessary to control the brazing time to ensure the diffusion of the brazing filler metal and base metal is complete while avoiding the formation of brittle compounds during the vacuum brazing of the borosilicate glass and Kovar alloy.

Figure 5 shows the typical fracture pattern of a sample measured using the tensile test. Figure 6 shows the rupture path of the brazed joint. The results indicate that the fracture occurs near the glass, and the shear rupture is cleavage fracture with little brittle fracture. Most microcracks propagate along the interface near the side of the glass, and sometimes micro cracks are close to the center of the interface. A similar situation occurs in samples using other sealing processes (Ref. 13). Large shear stress induced at the interface suppresses the crack propagation along the interface (Ref. 14). Residual thermal stresses within the joint are induced due to the CTE mismatch and different responses of the glass and the metal, which could weaken the brazed joint strength. Generally, the lower the thermal residual stresses are, the higher the allowable stress to the fracture of the joint (Ref. 15).

Microstructure of the Brazed Joint

The cross-section microstructure of the brazed joint is shown in Fig. 7. The cross section is divided into three regions marked by E, F, and G. The EDS analyses of the three regions are shown in Figs. 8, 9, and 10, respectively. As shown in Fig. 8, region E is near the copper-coated glass, which mainly consists of the elements Cu, Ni, Sn, and P. There is a zone enriching Cu and Sn near region F and region G — Fig. 9. However, P is not found. Therefore, Cu and Ni are prevented from forming Cu_3P and Ni_2P due to the decrease of P. As shown in Fig. 10, Au is found in the EDS analysis because of the gold spraying on the surface of the sample before EDS analysis, and region G is composed of Cu, Sn, Fe, and Ni. As we know, P can reduce the melting point of Cu filler metal and have a self-cleaning effect on the surface of metal. Phosphorus will react with the oxidation layer of the Kovar alloy and form P_2O_5 near the Kovar alloy side. Meanwhile, P has a high-vapor pressure and evaporates during brazing, which leads to enriching Cu and Sn near Regions

Table 3 — Thermal and Mechanical Properties of Borosilicate Glass and Kovar Alloy

Material	Temperature (K)	Young's Modulus (GPa)	Poisson's Ratio	CTE (10-6/K)	Yield Stress (MPa)
Borosilicate Glass		64	0.20	3.3	35~120
Kovar Alloy (4J29)	293	134	0.37	6.5	340
	473	141	0.37	5.9	200
	673	155	0.37	5.1	110

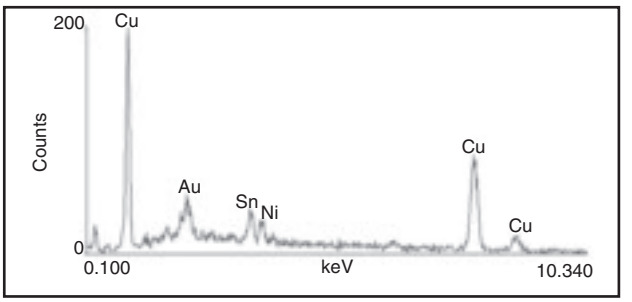

Fig. 9 — EDS analysis of a small area component of the brazing alloy (Region F).

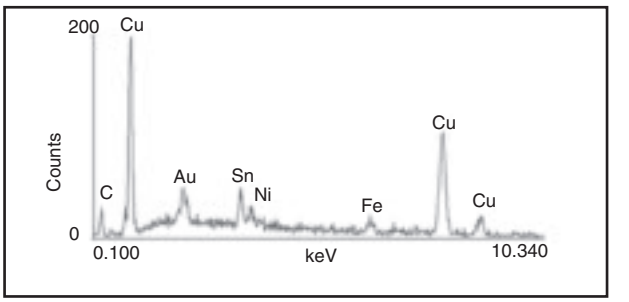

Fig. 10 — EDS analysis of a small area component of the brazing alloy-to-Kovar interface (Region G).

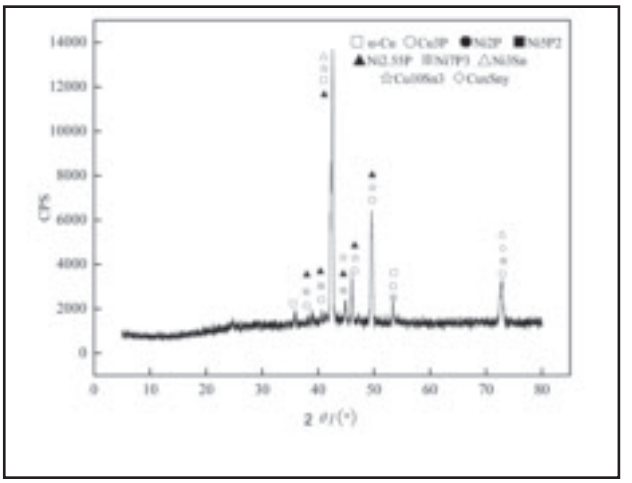

Fig. 11 — XRD patterns of the fracture interface.

F and G. However, P also diffuses with Cu near the copper-coated glass and forms Cu_3P and Ni_2P, besides partly evaporating. Cu_3P and Ni_2P are brittle compounds that reduce the mechanical strength of the brazed joints.

It can be seen that the metal element does not react with the glass. A reaction layer is necessary for adequate wettability of the filler metal on the copper-coated glass. However, the negative effect of the excessive growth of the reaction layer should also be considered. The formation of a brittle intermetallic in the condensed zone usually reduces the mechanical strength of the joint. The reaction layer should be thin and dense to inhibit further interaction between the reactive metals of the filler metal and the Kovar alloy as a diffusion barrier, which limits the formation of brittle phases.

According to XRD results (Fig. 11), the reaction products are mainly composed of α-Cu, Ni_2P, Cu_2P (or Cu_3P) and Cu_xSn_y. The mechanism of interface formation involving metallized glass differs from that of active filler metals. In metallized glass, Cu is already in contact with the glass surface, whereas the use of active filler metal requires the migration of Cu from the alloy to the glass.

Conclusions

Glass to metal was brazed at 943~973 K using Cu-Ni-Sn-P filler metal in vacuum, and shear strength tests and microstructure analyses were performed. The brazing process was optimized successfully. The main results are as follows:

1) The shear strength of the brazed joint depended on the brazing temperature and the brazing time. The shear strength reached 11.6 MPa when the brazing temperature and the brazing time were 680 K and 10 min, respectively.

2) The shear test results indicated that the fracture location of the brazed joint was near the side of the glass. Many microcracks occurred along the interface of the glass, then extended to the center of the interface.

3) It was determined that Cu_3P and Ni_2P intermetallic compounds, α-Cu, and Cu_xSn_y layer formed at the interface of the brazed joint. The brittle compounds Cu_3P and Ni_2P are mainly responsible for lowering the strength of the brazed joints.

Acknowledgments

The authors gratefully acknowledge the financial support rendered by the National Natural Science Foundation of China (Grant No. 10672072) and Hi-Tech Research Program Foundation of Jiangsu (Grant No. BG 2006040) in carrying out this investigation.

References

1. Zhang, Y. N., Liu, H., and Yuan, J. 2004. Sealing of glass to metal. *Glass & Enamel* 32(6): 34–37.

2. Susan, D. F., Van Den Avyle, J. A., Monroe, S. L., Sorensen, N. R., McKenzie, B. B., Christensen, J. E., Michael, J. R., and Walker, C. A. 2009. The effects of pre-oxidation and alloy chemistry of austenitic stainless steels on glass/metal sealing. *Oxidation of Metals* 73(1-2): 311–335.

3. Chanmuang, C., Naksata, M., Chairuangsri, T., Jain, H., and Lyman, C. E. 2008. Microscopy and strength of borosilicate glass-to-Kovar alloy joints. *Materials Science and Engineering* 474(1-2): 218–224.

4. Lagtenberg, R., Bouwstra, S., and Elwenspoek, M. 1991. Low temperature glass bonding for sensors applications using boron oxide films. *Journal of Micromechanics and Microengineering* 1: 157–160.

5. Wallis, G., and Pomerantz, D. I. 1969. Field-assisted glass-metal sealing. *Journal of Applied Physics* 40: 3946–3949.

6. Wallis, G. 1970. Direct current polarization during field-assisted glass-metal sealing. *Journal of the American Ceramic Society* 53(10): 563–567.

7. Lei, D. Q., Wang, Z. F., and Du., F. L. 2007. The glass-to-metal sealing process in parabolic trough solar receivers. *Proceedings of ISES World Congress*, Beijing: 740–744.

8. Shen, X. H., and Ling, X. 2008. Damage analysis of glass-to-metal diffusion welded joints. *Advanced Materials Research* 44-46: 765–772.

9. Xu, D., and Ling, X. 2008. Numerical simulation of residual stress in the glass-to-metal diffusion seals. *Materials Science Forum* 575-578: 666–671.

10. Zhang, B. W., Shu, X. L., Zhu, S. Y., and Liao, S. Z. 1999. Study on the thermal stability of Cu-P based amorphous alloy systems. *Journal of Materials Processing Technology* 91: 90–94.

11. Wang, Y., Feng, J. C., Zhang, L. X., He, P., and Zhang, J. H. 2007. Microstructure of alumina ceramic/Ag-Cu-Ti brazing alloy/Kovar alloy joint. *Materials Science and Technology* 23(3): 320–323.

12. Song, Y. W., Zhao, B., and Sun, C. X. 1999. Electroless copper plating and its application to glass industry. *Glass & Enamel* 27(5): 47–51.

13. Selcuk, A., Atkinson, A., and Senerveratne, D. 1999. Mechanical strength of glass-to-metal joints. *Metal Abstract* 32: 202–206.

14. Bartlett, A., Evans, A. G., and Ruhle, M. 1991. Residual stress cracking of metal/ceramic bonds. *Acta Metallurgica et Materialia* 39(7): 1579–1585.

15. Park, J. W., Mendez, P. F., and Eagar, T. W. 2002. Strain energy distribution in ceramic-to-metal joints. *Acta Materialia* 50(5): 883–899.